Contrib Mineral Petrol (1993) 113:572–581

Contributions to Mineralogy and Petrology
© Springer-Verlag 1993

# Thermodynamic and rheological properties of rhyolite and andesite melts

**Daniel R. Neuville[1], Philippe Courtial[1], Donald B. Dingwell[2], and Pascal Richet[1]**

[1] Institut de Physique du Globe, 4, place Jussieu, F-75252 Paris cedex 05, France
[2] Bayerische Geoinstitut, Universität Bayreuth, W-8580 Bayreuth, FRG

Received January 16, 1992/Accepted August 21, 1992

**Abstract.** The heat capacities of a rhyolite and an andesite glass and liquid have been investigated from relative-enthalpy measurements made between 400 and 1800 K. For the glass phases, the experimental data agree with empirical models of calculation of the heat capacity. For the liquid phases, the agreement is less good owing to strong interactions between alkali metals and aluminum, which are not currently accounted for by empirical heat capacity models. The viscosity of both liquids has been measured from the glass transition to 1800 K. The temperature dependence of the viscosity is quantitatively related to the configurational heat capacity (determined calorimetrically) through the configurational entropy theory of relaxation processes. For both rhyolite and andesite melts, the heat capacity and viscosity do not differ markedly from those obtained by additive modeling from components with mineral compositions.

## Introduction

It has long been acknowledged that igneous petrology relies on an adequate understanding of the composition and temperature dependences of the physical properties of silicate liquids (e.g., Bowen 1928). More recently, the density and viscosity models set up by Bottinga and Weill (1970, 1972) have demonstrated how the properties of real, complex magmas could be predicted from measurements performed on a limited number of simple systems. Beginning with Carmichael et al. (1977), systematic measurements have been made on geochemically relevant melts to extend the composition range of available physical data. Over wide temperature and composition domains, most properties have been found to vary in a way complex enough that empirical approaches are inappropriate to interpret the data.

The aim of this contribution is a first step in the extension to naturally occuring liquids of the experimental and theoretical methods we have developed recently for the viscosity and heat capacity of simple synthetic compositions. For this purpose, we have made calorimetric and viscosity measurements on a rhyolite and an andesite melt from the glass transition to superliquidus temperatures. Even though there is a fair amount of data for naturally occuring liquids, they generally do not span the wide temperature intervals covered in our study. Previous measurements made by Bacon (1977), Carmichael et al. (1977) and Murase and McBirney (1973) are exceptions in this respect; hence, it is mainly with these observations that we will compare our results. For both andesite and rhyolite compositions, we also discuss the manner in which the heat capacity and the viscosity are related to those of their oxide or mineral components. Finally, we relate the thermodynamic and rheological properties of the melts through the configurational entropy theory of relaxation processes (Adam and Gibbs 1965; Richet 1984; Richet and Neuville 1992), which provides a firm theoretical framework for consistent modeling of both kinds of melt properties.

The andesite and rhyolite are especially well suited for our purpose in view of the relative simplicity of their chemical compositions. Rhyolite compositions lie close to the ternary system $SiO_2$-$NaAlSi_3O_8$-$KAlSi_3O_8$, for which the properties of the end-members have been investigated previously (Taylor and Rindone 1970; Urbain et al. 1982; Richet et al. 1982; Richet and Bottinga 1984a). Even though andesite compositions are slightly more complex, they can be expressed in terms of these and $CaAl_2Si_2O_8$, $CaMgSi_2O_6$, and $FeSiO_3$ components. With the exception of $FeSiO_3$, the thermochemical and rheological properties of these components are also known (Bockris and Lowe 1954; Cukierman and Uhlmann 1973; Urbain et al. 1982; Richet and Bottinga 1984b, Neuville and Richet 1991).

## Experimental methods

The rhyolite and andesite samples are the materials previously investigated in a fiber-elongation study of silicate melt non-newtonian rheology (Webb and Dingwell 1990a). The rhyolite was

*Correspondence to:* P. Richet

prepared from a natural obsidian from Little Glass Butte (Oregon), which had an originally low water content of less than 0.2 wt.% as determined from Karl Fischer titration analyses. The andesite specimen was a synthetic sample. As described in detail by Webb and Dingwell (1990a), these materials were melted in Pt-alloy crucibles for a few days at high temperatures and stirred to obtain the bubble-free products required for the viscosity measurements. The amorphous nature of the quenched materials was checked through optical microscopy, X-ray diffractometry and transmission electron microscopy. Both andesite and rhyolite materials were found to be chemically homogeneous glassy phases before the calorimetry and viscosity measurements.

Electron microprobe analyses of the products (made in Bayreuth) are reported in Table 1. They agree with the analysis of rhyolite (made at CALTECH) and the nominal composition of andesite given by Webb and Dingwell (1990a). Numerous analyses were made to check possible differences in the alkali content of rhyolite. Within the uncertainties of the probe analyses, no significant differences have been found. Table 1 includes the molar masses, calculated from the molar fractions determined from the analyzed chemical compositions, as well as the number of atoms per formula unit which constitutes a useful framework for comparing the thermodynamic properties of related liquids.

We also determined the water content of the rhyolite material. With the calibration of Newman et al. (1986), infrared absorption measurements gave amounts of 6 and 5 ($\pm$ 2) ppm for the samples A and B of the high-viscosity measurements, respectively. For sample B, this number was confirmed by a vacuum fusion extraction which yielded a water content of 7 ppm, along with 4 ppm of $CO_2$. These low results conform to the volatile contents we have measured previously for a variety of silicate melts heated in air above 1800 K (unpublished results from the Paris laboratory).

The relative-enthalpy measurements ($H_T - H_{273.15}$) have been made with the ice calorimeters and the two different high-temperature setups described by Richet et al. (1982, 1992) working between 900 and 1800 K, and 400 and 1100 K, respectively. (Note that hereafter, we will abbreviate 273.15 as 273 K.) Measurements on sapphire indicate that the imprecision and inaccuracy of the measured enthalpies are usually less than 0.05 and 0.2%, respectively. The instrumental inaccuracy of the derived heat capacities is less than 0.5%. By taking into account uncertainties in the chemical compositions, errors of less than 1% are estimated for the reported molar heat capacities. About 5 g of material were run in PtRh 15% crucibles, the two 1.5-mm openings of which were rather tightly closed with crimped platinum foil, leaving less than 0.5 $cm^3$ of air in contact with the samples. The crucibles were heated in air and, to limit further possible changes in $Fe^{2+}/Fe^{3+}$ ratio, the heating period was kept as short as possible. In all cases, the sample spent less than 45 min above 1000 K. No significant weight variations of the materials, due to redox changes, were observed during the calorimetry measurements. After the drop, cooling of the crucible down to 273.15 K took about 20 min. The glass transition is a kinetic phenomenon which takes place at higher temperatures when the cooling rate is faster. The experiments described by Richet and Bottinga (1984a) indicate cooling rates of a few K/s through the glass transition in our experiments.

Viscosity measurements on stable liquids were performed in air with the concentric cylinder viscometer described by Dingwell (1989). Measurements on supercooled liquids were also made in air, with a fiber-elongation method, as described by Webb and Dingwell (1990b), and with the creep apparatus described by Neuville and Richet (1991). Within the range of stresses applied in the creep experiments, the viscosity of the samples was found to be Newtonian. Measurements were made with increasing or decreasing temperatures and no time dependence was observed during hour-long measurements. The reported values are thus relaxed viscosities, and their uncertainties are less than 0.02, 0.1 and 0.04 log units, respectively, for the three techniques. For the creep measurements on rhyolite, sample A was the same specimen as used in the drop-calorimetry and fiber-elongation experiments. Sample B was a specimen from another batch, whereas samples A1 and B2 were the same as A and B, respectively, but with a 360 h annealing at 1070 K in air prior to the viscosity measurements.

**Table 1.** Composition (wt.%) and related properties of the materials investigated[a]

| | Rhyolite | Andesite |
|---|---|---|
| $SiO_2$ | 77.90 (19) | 61.17 (15) |
| $Al_2O_3$ | 12.05 (17) | 17.29 (5) |
| MgO | 0.05 (1) | 3.35 (5) |
| CaO | 0.52 (2) | 5.83 (5) |
| $Na_2O$ | 4.01 (9) | 3.85 (6) |
| $K_2O$ | 4.06 (4) | 1.39 (2) |
| FeO | 0.76 (5) | 5.39 (19) |
| $TiO_2$ | 0.07 (2) | 0.84 (2) |
| $n$ | 3.139 | 3.050 |
| $gfw(g)$ | 64.373 | 64.478 |
| $d$ | 2.311 (4) | 2.533 (5) |

[a] Average of 15 analyses made with a Camebax electron microprobe for each material at 15 kV and 10 nA with a 15 s count time; total Fe as FeO; *gfw* is the gram formula weight on the basis of 1 mol of oxides, $n$ the number of atoms per *gfw*, and $d$ the glass room-temperature Archimedean density

## Calorimetry

### *Results*

The relative-enthalpy measurements are listed in Table 2. Runs are labelled in chronological order for each series of experiments. Observations made with the lower-temperature setup are indicated by the suffix B. Along with previous data, our results are also plotted in Figs. 1-2 in the form of mean heat capacities:

$$C_m = (H_T - H_{273})/(T - 273). \quad (1)$$

The slight temperature dependence of mean heat capacities permit illustration of the calorimetric data on an

**Table 2.** Relative enthalpy of amorphous rhyolite and andesite (kJ/gfw)

| | Rhyolite | | | Andesite | |
|---|---|---|---|---|---|
| Run | $T$(K) | $H_T - H_{273}$ | Run | $T$(K) | $H_T - H_{273}$ |
| DT.4-B | 416.0 | 7.810 | EO.1-B | 433.1 | 8.608 |
| DT.2-B | 603.1 | 19.914 | EO.6-B | 558.2 | 16.663 |
| DT.3-B | 808.0 | 34.525 | EO.2-B | 626.8 | 21.347 |
| CK.13 | 941.9 | 44.568 | EO.5-B | 729.5 | 28.619 |
| CK.3 | 977.1 | 47.249 | DS.10-B | 777.8 | 32.075 |
| CK.4 | 1017.1 | 50.326 | EO.4-B | 823.9 | 35.476 |
| CK.5 | 1064.5 | 53.803 | EO.3-B | 893.7 | 40.738 |
| CK.17 | 1091.4 | 55.969 | DS.11-B | 916.5 | 42.363 |
| CK.6 | 1119.8 | 58.227 | DS.1 | 960.5 | 45.689 |
| CK.18 | 1162.3 | 61.584 | DS.14 | 1038.1 | 52.067 |
| CK.7 | 1176.3 | 62.846 | DS.12 | 1060.4 | 53.930 |
| CK.8 | 1272.9 | 70.909 | DS.6 | 1081.8 | 55.780 |
| CK.19 | 1286.7 | 72.045 | DS.3 | 1116.1 | 59.123 |
| CK.15 | 1442.5 | 85.091 | DS.19 | 1383.1 | 83.210 |
| CK.16 | 1569.9 | 95.902 | DS.18 | 1414.7 | 86.265 |
| CK.9 | 1670.0 | 104.730 | DS.16 | 1445.4 | 88.980 |
| CK.12 | 1767.4 | 113.470 | DS.13 | 1472.7 | 91.671 |
| | | | DS.8 | 1507.9 | 95.031 |
| | | | DS.17 | 1627.3 | 105.89 |

expanded scale, without the fitting bias that can beset the derived heat capacities. For comparison, we have included in Figs. 1–2 the $H_T - H_{300}$ data reported by Bacon (1977) and Carmichael et al. (1977) for other rhyolite and andesite compositions. In both cases, the model of Richet (1987) was used to calculate $H_{300} - H_{273}$ in order to refer these data to the same reference temperature of 273 K as in our measurements.

As discussed later, the heat capacity of silicates above room temperature is of the order of the Dulong-and-Petit limit of $3R/g$ atom, where $R$ is the gas constant. This is the reason why heat capacities and enthalpies are properties depending primarily on the number of atoms of the formula unit. Since extensive thermodynamic properties can be expressed in a variety of ways for rock compositions, we have plotted the calorimetric data on a $g$ atom basis in Figs. 1–2 from the numerical results reported on a gfw basis in Tables 2 and 3 and the number of atoms per gfw included in Table 1. In this way, differences in numbers of atoms per gfw between related compositions are automatically accounted for, and the differences between our results and those of Bacon (1977) and Carmichael et al. (1977) are smaller than when all data sets are compared on a J/g or J/gfw basis.

The main feature of Figs. 1–2 is the change in the slope of the $C_m$ curves found at temperatures of about 1100 and 1000 K for the rhyolite and andesite compositions, respectively. This is the signature of the marked heat capacity discontinuity at the glass to liquid transition. For each composition, two different enthalpy equations for the glass and liquid phases have thus to be fitted to the enthalpy data. We used empirical equations of the form:

$$H_T - H_{273} = R_{273} + aT + bT^2/2 - c/T + 2dT^{0.5}. \quad (2)$$

These equations were differentiated to yield the heat capacities of the glasses and liquids:

$$C_p = a + bT + c/T^2 + d/T^{0.5}, \quad (3)$$

which are plotted as a function of temperature in Figs. 3–4.

For the glasses, the constant $R_{273}$ of Eq. (2) is determined by the $a, b, c$ and $d$ parameters through the constraint $H_T - H_{273} = 0$ for $T = 273$ K, whereas it is an adjustable parameter for liquids whose enthalpy equation does not extrapolate to 0 at 273 K. The parameters of Eqs. (2–3) are listed in Table 3, along with the average absolute deviations of the fitted values from the measurements of Table 2. The glass transition temperatures listed in Table 4 were taken as the temperatures at which the enthalpy equations of the liquids intersect those of the glasses. It is observed that the $C_p$ increases at the glass transition vary sympathetically with decreasing $SiO_2$ contents (e.g., Richet and Bottinga 1984a, b). The sharper glass transition observed for andesite with respect to rhyolite melt conforms to this trend.

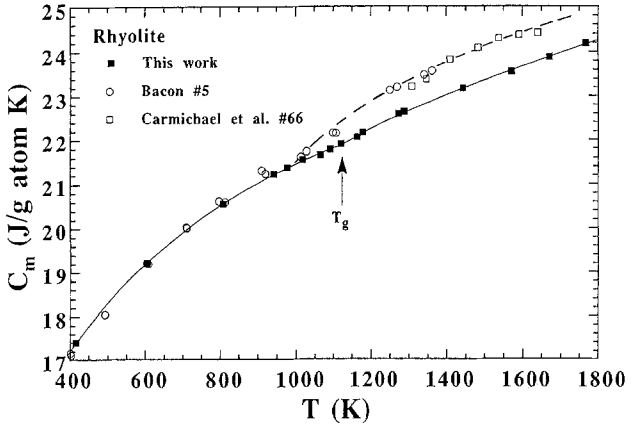


**Fig. 1.** Mean heat capacity of rhyolite glass and liquid. Measurements of Table 2 (errors smaller than the *solid squares*) and data for compositions no. 5 of Bacon (1977) and no. 66 of Carmichael et al. (1977). The glass transition temperatures are indicated by the *arrows*. The *solid curves* are values given by the fitted data of Table 3, whereas the *dashed curve* is a visual fit to the Berkeley data

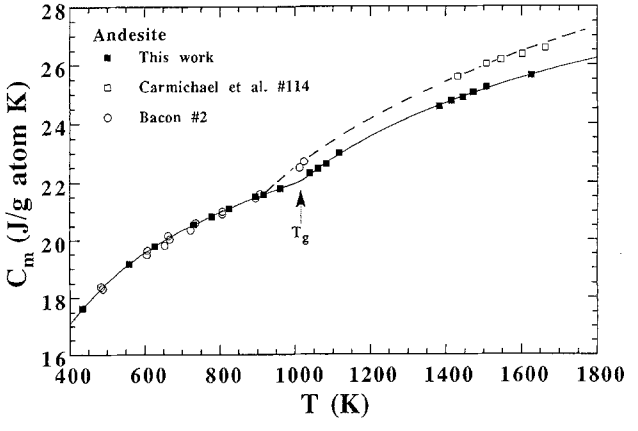


**Fig. 2.** Mean heat capacity of andesite glass and liquid. Measurements of Table 2 and data for compositions no. 2 of Bacon (1977) and no. 114 of Carmichael et al. (1977). Same comments as in Fig. 1 caption

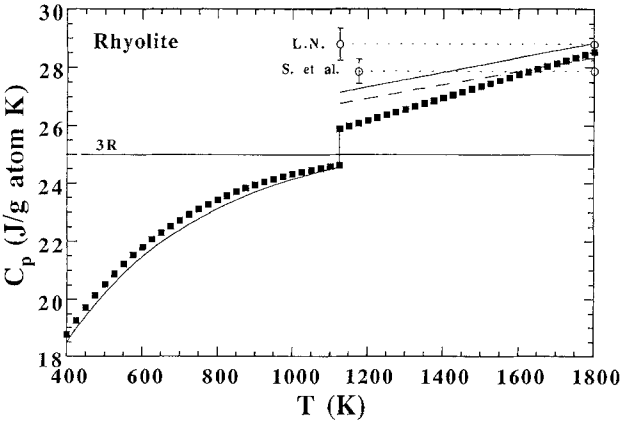


**Fig. 3.** Heat capacity of rhyolite glass and liquid. The *solid squares* are the values given by the $C_p$ equations of Table 3. The *solid curves* represent the model values of Richet (1987) and Richet and Bottinga (1985) for the glass and liquid, respectively, and the *dashed curve* the sum of the heat capacities of the molten mineral components taken as $SiO_2$ (0.39 mol) $NaAlSi_3O_8$ (0.086) and $KAlSi_3O_8$ (0.056), see text. The *dotted lines* with the labels S. et al. and L.N. show the temperature independent model heat capacities of Stebbins et al. (1984) and Lange and Navrotsky (1992)

**Table 3.** Coefficients of $C_p = a + bT + c/T^2 + d/T^{1/2}$ (J/gfw K) and $H_T - H_{273} = R_{273} + \int C_p dT$ (J/gfw)

| | $a$ | $10^3 b$ | $10^{-5} c$ | $d$ | $R_{273}$ | $\Delta T$ (K) | AAD[a] |
|---|---|---|---|---|---|---|---|
| Rhyolite glass | 140.30 | − 14.22 | 6.37 | − 1594.1 | | 416–1119 | 0.06 |
| liquid | 67.51 | 12.24 | | | − 25039. | 1162–1767 | 0.08 |
| Andesite glass | 68.062 | 10.698 | − 21.398 | 0 | | 433–961 | 0.06 |
| liquid | 83.555 | 6.0589 | | | − 38025. | 1038–1627 | 0.13 |

[a] AAD is the average absolute deviations of the fitted values from the experimental data

**Table 4.** Heat capacity increase at the glass transition, and configurational heat capacity coefficients, $C_p^{conf} = a + bT$ (J/g atom K)

| | $T_g$(K) [a] | $C_{pg}(T_g)$ | $C_{pl}(T_g)$ | $\Delta C_p$(%) | $a$ | $10^3 b$ |
|---|---|---|---|---|---|---|
| Rhyolite | 1125 | 24.65 | 25.89 | 5 | − 3.10 | 3.90 |
| Andesite | 1013 | 25.18 | 29.41 | 17 | 2.21 | 1.99 |

[a] $T_g$ is the glass transition temperature as given by the intersection of the relative-enthalpy equations of the glass and liquid phases

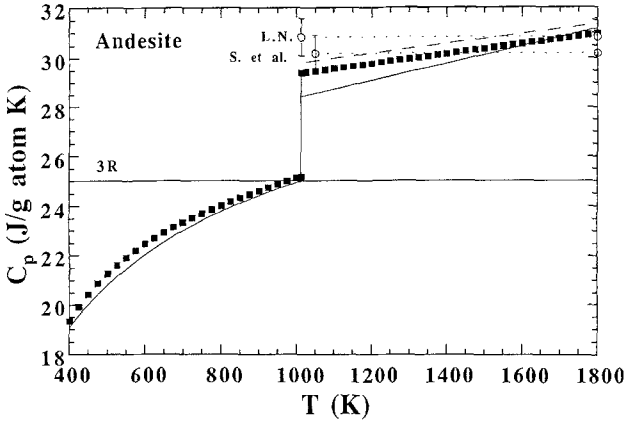


**Fig. 4.** Heat capacity of andesite glass and liquid. Same comments as in Fig. 4 caption. Mineral components taken as $SiO_2$ (0.13 mol) $NaAlSi_3O_8$ (0.081), $KAlSi_3O_8$ (0.019), $CaAl_2Si_2O_8$ (0.06), $CaMgSi_2O_6$ (0.015) $MgSiO_3$ (0.047) and $FeSiO_3$ (0.049)

*Heat capacity of glasses*

Below the glass transition, our results are consistent with those of Bacon (Figs. 1–2). The differences of about 1% or less are within the combined errors of the measurements. This good agreement between Bacon's data and our results shows that minor composition differences such as variations in ferrous-ferric ratios do not have significant effects on the heat capacity of rhyolite and andesite glasses. By referring $C_p$ to g atom amounts, one could use the data of Table 3 as a basis for predicting the heat capacity of related compositions. A more general approach should be used, however, through available models of calculation of the heat capacity of silicate glasses from partial molar heat capacities of oxide components. As shown in Figs. 3–4, the values predicted by the model of Richet (1987) agree to within 1–1.5% with the values given by the data of Table 3. Similar results are obtained for the heat capacity with the model of Stebbins et al. (1984), but this model is valid only for temperatures higher than 400 K and it cannot be used for calculating relative enthalpies down to room temperature.

*Heat capacity of liquids*

Materials and calorimetric equipment were apparently the same in the investigations of Bacon (1977) and Carmichael et al. (1977), which were both performed in Berkeley on the same base samples. The main difference dealt with the oxidation state of iron, which was mainly ferrous in the former and ferric in the latter study. The consistency of the results from these studies would suggest that the effect of oxidation on the heat capacity is slight and cannot account for the differences shown in Figs. 1–2 between our results and the Berkeley measurements, which reach about 3% at 1800 K for the relative enthalpies of both rhyolite and andesite melts. However, such an effect could be partly concealed by the unreported "small temperature-dependent correction" applied by Carmichael et al. (1977) to their measurements on stable liquids to join smoothly with their measurements made at lower temperatures.

The glass transition temperature (at constant cooling rate) is found to depend very sensitively on impurity content for $SiO_2$-rich aluminosilicates, whereas no strong effects on the heat capacity of the liquid are observed (see Richet and Bottinga 1984a). Because the heat capacity of a liquid is higher than that of a glass, measured relative enthalpies for liquids are higher for samples with lower glass transition temperatures. For two samples of a given material undergoing the glass transition at different temperatures $T_{g1}$ and $T_{g2}$, this enthalpy difference is:

$$\Delta H_a = \int_{T_{g2}}^{T_{g1}} \Delta C_p dT, \tag{4}$$

where $\Delta C_p$ is the heat capacity difference between the liquid and glass. The glass transition is not precisely defined by the data of Bacon (1977) and Carmichael et al. (1977), but inspection of the data plotted in Figs. 1–2 suggest that it took place at temperatures about 100 K lower than for our rhyolite and andesite samples. With Eq. (4), the resulting enthalpy differences are calculated as 0.46 and 1.8 kJ/gfw for rhyolite and andesite liquid, respectively. Hence, part of the discrepancy between our results and those of Bacon (1977) and Carmichael et al. (1977) likely results this effect, but the composition dependence of the glass transition is unfortunately not well enough known to allow $T_g$ predictions. On the other

hand, comparisons between our data (Richet et al. 1982) and those of Bacon for sapphire suggest that the Berkeley results become too high with increasing temperatures, by about 1–2% at the highest temperatures. Likewise, similar differences between these laboratories have also been reported for other liquids (e.g., $CaAl_2Si_2O_8$, Stebbins et al. 1982; Richet and Bottinga 1984b). The rest of the discrepancy thus probably originates in systematic differences in the measurements.

At the highest experimental temperatures, the heat capacities of rhyolite and andesite liquids are similar (Figs. 3–4). In contrast to andesite melts, rhyolite liquids have strongly temperature dependent heat capacities. As a result, the heat capacity of liquid rhyolite is smaller than that of andesite at lower temperatures, and so is the $C_p$ increase at the glass transition. Stebbins et al. (1984) and Lange and Navrotsky (1992) have set up empirical models for predicting the heat capacity of stable silicate liquids from partial molar heat capacities of oxide components that are temperature and composition independent. Comparison of the values calculated from these models with the experimental data of Figs. 3–4 shows fair agreement at the highest temperatures. Of course, these models cannot account for the experimentally observed temperature dependence of the heat capacity. For instance, they overestimate the heat capacity of supercooled rhyolite liquid at 1200 K by 6 and 10%, respectively. This is worrisome because accurate data are especially needed at subliquidus temperatures for phase equilibria calculations.

That $C_p$ is generally temperature dependent for aluminosilicate liquids was emphasized in the heat capacity model of Richet and Bottinga (1985). But the measurements available at that time did not allow correct modeling of $C_p$ as a function of composition, and Richet and Bottinga added an approximate average value for $Al_2O_3$ to a set of partial molar heat capacities for oxides in Al-free liquids. Because the temperature dependence of $C_p$ is greater for alkali than for alkaline-earth aluminosilicates, the deviations of the model values from the experimental data differ for andesite and rhyolite. For andesite, the calculated values are 1% too high at 1800 K and 4% too low at 1200 K. For rhyolite, they are 1 and 4% too high at 1800 K and 1200 K, respectively. Additional measurements are thus required in order to derive a nonideal heat capacity model based on oxide components which will be really satisfactory from the glass transition to magmatic temperatures.

The significant composition dependence of the heat capacity of silicate melts is embodied in available measurements for simple compositions. As a matter of fact, molten alkali feldspar and plagioclases have heat capacities that are similar to those of rhyolite and andesite liquids, respectively (Richet and Bottinga 1984a, b). This suggests that a simpler and currently more accurate way of calculating the heat capacity of these liquids would consist of summing up appropriately values for components having mineral compositions. With available data (Richet et al. 1982; Richet and Bottinga 1984a, b) and calculated values for $MgSiO_3$ and $FeSiO_3$ (Richet and Bottinga 1985), one obtains the values shown in Figs. 3–4 which agree better with the measurements even though the discrepancy is still slightly higher than the experimental errors for rhyolite melt. This is another evidence for the complex behavior of alkali-aluminosilicate liquids with respect to heat capacity.

### *Configurational heat capacity*

For both rhyolite and andesite compositions, the glass transition takes place when the heat capacity of the glasses is close to the Dulong-and-Petit harmonic limit of $3R$/g atom. In this respect, they behave as all other silicate glasses investigated so far (e.g., Richet and Bottinga 1986). For silicate liquids, the configurational heat capacity can be approximated by the difference between the heat capacity of the liquid and that of the glass at the glass transition temperature (Richet et al. 1986):

$$C_p^{\text{conf}} = C_{pl} - C_{pg}(T_g). \tag{5}$$

Hence, $C_p^{\text{conf}}$ is seen in Figs. 3–4 as the difference between $C_{pl}$ and the horizontal line plotted for $3R$. Just above the glass transition, the configurational heat capacity of rhyolite and andesite melts is about 5 and 17% of the glass $C_p$, respectively (Table 4), and it is the strong increase with temperature of $C_p$ for liquid rhyolite which brings its $C_p^{\text{conf}}$ to a value similar to that of andesite liquid. In this respect, liquid rhyolite behaves like $SiO_2$, $NaAlSi_3O_8$ and $KAlSi_3O_8$ liquids, which all show only slight heat capacity increases at the glass transition (e.g., Richet and Bottinga 1984a). Likewise, the $C_p$ increase of liquid andesite is intermediate between the small values found for $SiO_2$ and $NaAlSi_3O_8$ and the much greater numbers observed for $CaAl_2Si_2O_8$ and pyroxene components (Richet and Bottinga 1984b). These trends conform to the structural changes reported for these systems (e.g., Mysen 1988).

## Viscosity

### *Andesite*

The viscosity measurements are listed in Table 5. The low-temperature measurements were made with the creep apparatus only. Different samples gave the same results, but it was observed that the viscosity was increasing with time in a very long experiment (Fig. 5). Electron-microscopy observations showed that the initially homogeneous material had developed tiny opaque globules about 100 Å

**Table 5.** Viscosity of andesite melt (poise)

| $T$(K) | log $\eta$ | $T$(K) | log $\eta$ |
|---|---|---|---|
| 939.3 | 13.66 | 1670.0 | 3.19 |
| 950.6 | 13.30 | 1719.0 | 2.97 |
| 961.7 | 12.85 | 1768.0 | 2.74 |
| 971.8 | 12.64 | 1818.0 | 2.52 |
| 981.1 | 12.33 | 1867.0 | 2.33 |
| 992.2 | 11.83 | | |
| 1011.8 | 11.25 | | |
| 1025.5 | 10.90 | | |
| 1036.8 | 10.67 | | |

in diameter after a 24-h annealing at 1002 K in air. No chemical analysis of these inclusions could be made with the analytic electron microscope because of their very small size, and Mössbauer spectroscopy could not be performed on the same sample because the material had become paramagnetic. This observation suggests that the inclusions consist primarily of magnetite, as those previously observed by Regnard et al. (1981) in oxidized obsidians. The volume fraction of the inclusions is negligible and their growth cannot account for the increase in viscosity with time (Lejeune and Richet 1991). It is likely that these variations result from progressive oxidation of ferric to ferrous iron in the bulk of the liquid during the measurements, of which magnetite crystallization is just a consequence. This would agree with the observations of Klein et al. (1983) on iron-bearing aluminosilicates who demonstrated that the viscosity increases as a melt becomes more oxidized.

*Rhyolite*

For rhyolite, four different samples have been investigated with the creep apparatus whereas only one specimen was studied with the fiber-elongation method. These measurements are listed in Table 6. No time dependence analogous to that shown in Fig. 5 was observed during the measurements of the viscosity of the various samples, which lasted a total of five to ten hours for a given sample. The results have the usual precision for a given sample, but the comparison of Fig. 6 shows a range of 0.5 log units spanned by the viscosities of the various samples. A difference of about 0.25 log units has been found previously for $CaMgSi_2O_6$ between the data of Webb and Dingwell (1990b) and those of Neuville and Richet (1991). Most of the difference of about 0.4 log units found between the fiber-elongation and creep measurements for the as-quenched samples A and D (Table 6) thus likely originates in the different experimental techniques.

However, it remains to explain the difference of 0.3 log units between samples A and B, and for the 0.3 log units increase in viscosity observed for these samples after a 360 h annealing in air at 1070 K. The scatter in the data of Fig. 6 translates to temperature differences of less than 40 K. It is well known that the viscosity of molten $SiO_2$ and alkali feldspar compositions vary very strongly with minor composition differences (e.g., Leko 1979). In the same way, addition of 1 wt.% $H_2O$ has been found to reduce the viscosity of an initially anhydrous obsidian by two orders of magnitude (Shaw 1963). As noted, however, no significant differences in chemical composition could be detected by electron microprobe analyses, and the same very low water content was found for samples A and B. Hence, we cannot state which difference in impurity content is responsible for the difference between samples A and B. As to the influence of annealing, we surmise that

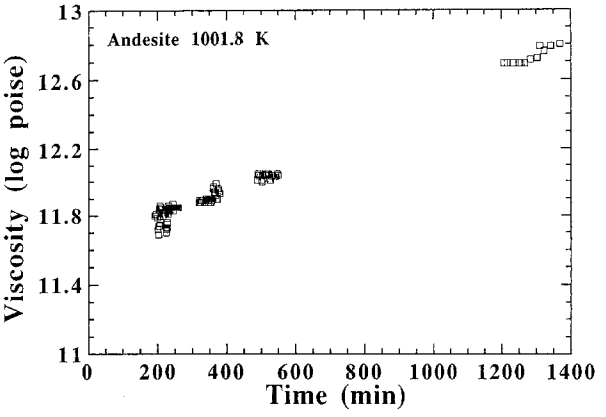


**Fig. 5.** Variation with time of the low-temperature viscosity of an andesite sample in air. Initial sample dimensions: 4.7 ×4.4 ×5.5 mm

**Table 6.** Viscosity of rhyolite melt (poise)

| Sample A[a] | | Sample B | | Sample A1[b] | | Sample B1[c] | | Sample D[d] | | | |
|---|---|---|---|---|---|---|---|---|---|---|---|
| $T$(K) | log $\eta$ | $T$(K) | log $\eta$ | $T$(K) | log $\eta$ | $T$(K) | log $\eta$ | $T$(K) | log $\eta$ | $T$(K) | log $\eta$ |
| 1088.0 | 12.22 | 1051.0 | 13.10 | 1096.9 | 12.37 | 1098.3 | 12.56 | 920. | 16.08 | 1670.0 | 5.79 |
| 1089.2 | 12.06 | 1070.6 | 12.92 | 1097.6 | 12.34 | 1110.6 | 12.37 | 988. | 14.77 | 1719.0 | 5.41 |
| 1094.2 | 11.86 | 1081.3 | 12.81 | 1106.8 | 12.18 | 1120.3 | 12.21 | 1063. | 13.49 | 1768.0 | 5.09 |
| 1110.9 | 11.76 | 1100.6 | 12.34 | 1120.3 | 11.92 | 1134.5 | 11.93 | 1068. | 13.26 | 1817.0 | 4.81 |
| 1110.9 | 11.76 | 1098.4 | 12.27 | 1126.1 | 11.81 | 1151.3 | 11.65 | 1091. | 12.87 | 1867.0 | 4.50 |
| 1126.8 | 11.50 | 1111.1 | 12.05 | 1130.5 | 11.77 | 1166.1 | 11.36 | 1094. | 12.51 | 1916.0 | 4.22 |
| 1144.8 | 11.24 | 1126.9 | 11.89 | 1134.5 | 11.66 | 1175.7 | 11.18 | 1128. | 12.02 | | |
| 1145.1 | 11.20 | 1127.2 | 11.73 | 1134.7 | 11.63 | 1190.2 | 10.95 | 1129. | 12.02 | | |
| 1171.3 | 10.81 | 1167.4 | 11.19 | 1146.9 | 11.42 | 1204.5 | 10.74 | 1131. | 11.92 | | |
| 1192.7 | 10.49 | 1193.5 | 10.78 | 1155.1 | 11.31 | 1219.1 | 10.54 | 1135. | 11.87 | | |
| 1210.5 | 10.23 | | | 1156.3 | 11.30 | 1230.8 | 10.36 | 1136. | 11.90 | | |
| 1225.5 | 10.03 | | | 1167.1 | 11.15 | | | 1138. | 11.84 | | |
| | | | | 1177.1 | 10.99 | | | 1157. | 11.62 | | |
| | | | | 1194.1 | 10.73 | | | 1186. | 11.07 | | |
| | | | | 1213.3 | 10.36 | | | 1219. | 10.55 | | |
| | | | | | | | | 1221. | 10.57 | | |
| | | | | | | | | 1253. | 10.19 | | |

[a] Same sample as in drop-calorimetry measurements
[b] Same sample as A, with a 360 hour annealing at 1070 K
[c] Same sample as B, with a 360 hour annealing at 1070 K
[d] Sample investigated in fiber-elongation measurements

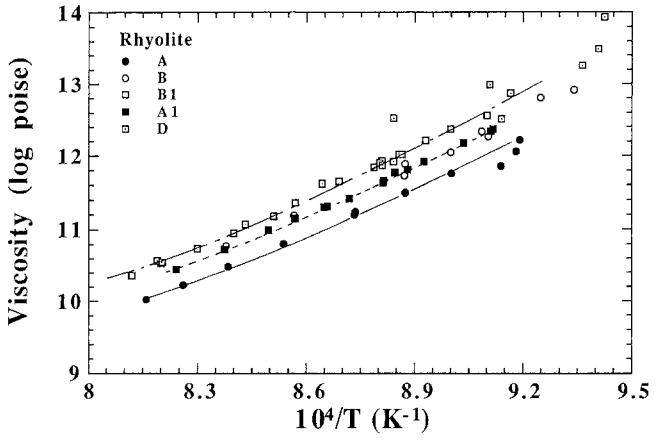


**Fig. 6.** Low-temperature viscosity of liquid rhyolite. The labels refer to the various samples investigated by creep (*A*, *B*, *A*1 and *B*1) and by fiber-elongation (*D*) measurements (see Table 6)

partial oxidation of iron during the annealing could account for the viscosity increase even though the iron content of rhyolite is small. (In this respect, relaxation problems can be ruled out because all viscosities would converge at the highest temperatures investigated, instead of following the subparallel curves of Fig. 6).

*Temperature dependence of the viscosity*

The high- and low-viscosity measurements listed in Tables 5–6 are plotted in Figs. 7–8 as a function of reciprocal temperature, along with data for simple related liquids when available over the same wide viscosity ranges. Overall, these measurements are beset to some extent by changes in the $Fe^{2+}/Fe^{3+}$ ratio, which generally increases with temperature at constant oxygen fugacity. Empirical redox models (e.g., Kress and Carmichael 1988) indicate that both of our rhyolite and andesite liquids have about the same amounts of $Fe^{2+}$ and $Fe^{3+}$ at around 1800 K and suggest that at equilibrium our samples would have only a few percent total ferrous iron at the glass transition temperature. The slow rate at which the viscosity was increasing with time (Fig. 5) shows, however, that the measurements reported in Tables 5–6 represent data at essentially constant $Fe^{2+}/Fe^{3+}$ ratios, i.e., those frozen-in during the initial quench of the products. At higher temperatures, the redox kinetics is fast enough that the viscosity data unlikely refer to constant compositions. But the effect on the viscosity should be small in view of the relatively small amounts of iron in andesite and especially rhyolite, combined to the influence of the oxygen fugacity of the viscosity of Fe-rich melts at high temperatures which is a matter of 0.5 log units only (e.g., Dingwell and Virgo 1987).

Over the temperature interval investigated, the viscosity of andesite clearly shows a non-Arrhenian nature, i.e., the viscosity does not vary linearly as a function of reciprocal temperature. For rhyolite, this non-Arrhenian behavior is much less pronounced and probably blurred by the scatter in the low-temperature measurements and the entropy of mixing effect discussed below. Empirically, these

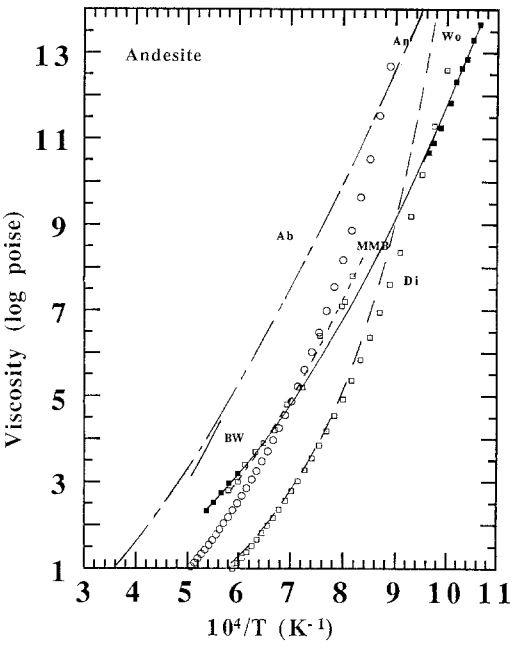


**Fig. 7.** Viscosity of andesite and related melts. *Solid squares*: data of Table 5. *BW*, model calculations of Bottinga and Weill (1972); *MMB*, Murase and McBirney (1973); *Ab*, $NaAlSi_3O_8$ (Taylor and Rindone 1970; Urbain et al. 1982); *An*, $CaAl_2Si_2O_8$ (Cukierman and Uhlmann 1973); *Di*, $CaMgSi_2O_6$ (Urbain et al. 1982; Neuville and Richet 1991); *Wo*, $CaSiO_3$ (Bockris and Lowe 1954; Neuville and Richet 1991)

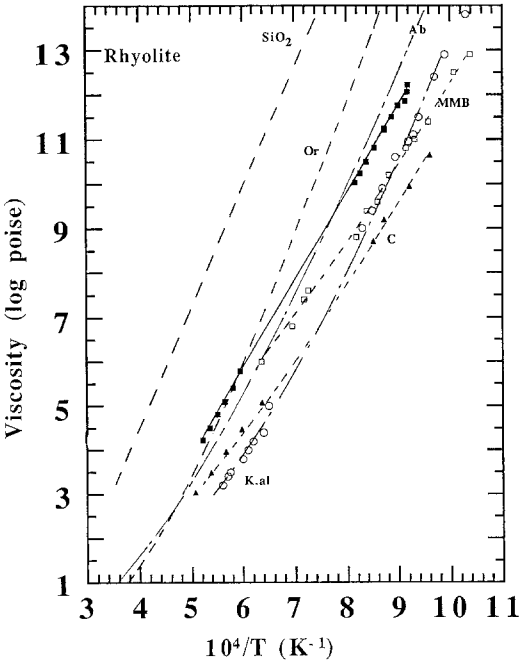


**Fig. 8.** Viscosity of rhyolite and related melts. *Solid squares*: data of Table 6, sample A. *C*, Carron (1969); *K.al*, Klein et al. (1983); *MMB*, Murase and McBirney (1973); *Ab*. same as in Fig. 7; $SiO_2$, and *Or* $KAlSi_3O_8$ (Urbain et al. 1982)

variations with temperature can be accounted for with the Tammann-Vogel-Fulcher equation:

$$\log \eta = A + B/(T - T_1), \tag{6}$$

where $A$, $B$ and $T_1$ are adjustable parameters listed in

**Table 7.** Coefficients of the viscosity equations (6) and (7–8) [a]

| | Eq. (6) | | | | | | Eq. (7–8) | | |
|---|---|---|---|---|---|---|---|---|---|
| | $A$ | $10^{-3}B$ | $T_1$ | $\sigma_\eta$ | $T_g$ | $S^{conf}(T_g)$ | $A_e$ | $10^{-5}B_e$ | $\sigma_\eta$ |
| Rhyolite | − 5.88 | 19.181 | 22.3 | 0.05 | 1125 | 3.12 | − 0.6014 | 0.4247 | 0.05 |
| Andesite | − 2.97 | 7.185 | 508.7 | 0.05 | 1013 | 3.19 | − 1.0827 | 0.3996 | 0.05 |

[a] The temperature $T_{13}$ is arbitrarily chosen as the temperature at which the viscosity is $10^{13}$ poise, as given by Eq. (6); m$\sigma_\eta$ is the standard deviation of the fitted viscosities in log units; $S^{conf}(T_g)$ is the configurational entropy at the calorimetric glass transition temperature; other data reported in K, J, and g atom

Table 7. For the sake of consistency between the calorimetry and viscosity measurements, the parameters of Table 7 were obtained for rhyolite from the low-temperature data of Table 6 for sample A only, which were combined with the high-temperature results.

For viscosity measurements, a glass transition temperature $T_{13}$ may be arbitrarily defined as the temperature at which the viscosity is $10^{13}$ poise, i.e., 1038 and 959 K for rhyolite and andesite, respectively, from the parameters of Eq. (6). These temperatures are 87 and 54 K lower than the calorimetric temperatures of Table 4 which refer to the fast quench rates of the drop calorimetry measurements. As expected, this difference shows that the relaxation times derived from a Maxwell relaxation for a viscosity of $10^{13}$ poise are longer than those at the calorimetric glass transition. At these calorimetric glass transition temperatures, the enthalpy relaxation times should be the same, whereas the viscosity of our andesite and rhyolite samples are $10^{11.5}$ and $10^{10.9}$ poises, respectively, which is close or within the range $10^{11.7\pm0.5}$ poise delineated by previous measurements reviewed by Neuville and Richet (1991) for other silicate compositions.

## Configurational Entropy

The difference between the viscosity of andesite and rhyolite liquids is readily accounted for through the configurational entropy theory of relaxation processes (Adam and Gibbs 1965; Richet 1984). The basic idea is that viscous flow takes place through a cooperative rearrangement of the configuration of a liquid. A liquid with a zero configurational entropy would have an infinite viscosity since only one configuration would be available. In contrast, when the configurational entropy ($S^{conf}$) increases, the structural rearrangements needed for viscous flow can take place in smaller and smaller regions of the liquid: the viscosity thus decreases when the temperature increases. Quantitatively, one predicts for the viscosity:

$$\log \eta = A_e + B_e/TS^{conf}, \tag{7}$$

where $A_e$ is a pre-exponential term and $B_e$ is the Gibbs free energy hindering the structural rearrangement in the liquid. The temperature dependence of the configurational entropy is given by:

$$S^{conf}(T) = S^{conf}(T_g) + \int_{T_g}^{T} C_p^{conf}/T\, dT. \tag{8}$$

If one takes the calorimetric glass transition temperature $T_g$ as the reference temperature in Eq. (7), then $S^{conf}(T_g)$ represents the residual entropy of the glass at 0 K which has been frozen in at the glass transition. For some simple compositions, this entropy can be determined by calorimetric methods from measurements which include that of the entropy of fusion of the crystalline form of the material (e.g., Richet 1984). For compositions like andesite and rhyolite, this is not possible and $S^{conf}(T_g)$ becomes a third adjustable parameter in Eqs. (7–8).

The parameters of Eqs. (7–8) listed in Table 7 were obtained from the same viscosity data used to determine the empirical parameters of Eq. (6). From Eqs. (7–8), it is clear that deviations from Arrhenian behavior (e.g., $B_e/S^{conf}$ = constant) increases with the magnitude of $C_p^{conf}$. This is the reason for the much stronger deviations from Arrhenian variations observed for andesite with respect to rhyolite melt. For rhyolite, a strong correlation exists between the inferred $S^{conf}(T_g)$ and the parameter $B_e$ because of the quasi-Arrhenian variation of the viscosity. Calculations with a range of entropy values showed, however, that a lower bound could be safely obtained for $S^{conf}(T_g)$, below which the viscosity data could not be reproduced to within their error margins. This value has been reported in Table 7.

## Discussion

Our thermochemical measurements confirm that the heat capacity and relative enthalpy of silicate glasses can be accurately estimated with empirical coefficients for oxide components which are additive functions of composition. The situation is less satisfactory for liquids because of the strong interaction between alkali elements and aluminum, which results in complicated temperature and composition dependences of the heat capacity. Available models of prediction of $C_p$ give results that are correct for alkali-poor aluminosilicate melts only. At this moment, these problems can be partly obviated either by assuming additivity of the heat capacity of mineral components, or by using the present results on rhyolite and andesite liquids as master curves from which the properties of other compositions can be obtained on a g atom basis. But more measurements on simple systems are required to establish a general model of prediction of the heat capacity of melts of geochemical interest. Determining the relative enthalpy between the melt at magmatic temperature and the glass at room temperature requires, in addition, specification of the temperature at which the glass transition takes place. Of course, the glass transition temperature depends on the cooling rate, but this effect is probably minor for $SiO_2$-rich compositions with respect to the influence of composition which is not predictable yet.

Since the glass transition temperature scales closely with the viscosity, understanding the way the glass transition depends on composition is tantamount to understanding the composition dependence of the viscosity near the glass transition range. At high temperatures, the main features of these variations are generally accounted for by the empirical model of Bottinga and Weill (1972). For our andesite sample, for instance, this model predicts viscosities one order of magnitude higher than the measurements of Table 5 (Fig. 7). But this model does not extend to temperatures lower than 1500 K and melts with more than 80 mol% $SiO_2$. In fact, available data show that the composition dependence is the strongest at high viscosities (see Fig. 1 of Richet 1984, for example). This is also apparent in Figs. 7–8 where we have plotted data available over wide viscosity ranges for melts with compositions not too different from those of our andesite and rhyolite samples. The difference between the andesite data of Murase and MacBirney (1973) and ours is slight at low viscosity and becomes significant at viscosities higher than $10^5$ poise. Likewise, most of the rhyolite data plotted in Fig. 8 converge at high temperatures after having spanned four orders of magnitude near the glass transition. All these data thus illustrate how misleading can be low-temperature extrapolations of high-temperature data.

The configurational entropy theory is successful at accounting for both the temperature and composition dependence of the viscosity for simple systems (e.g., Richet 1984; Hummel and Arndt 1985; Neuville and Richet 1991). But the data available at high viscosities are not yet sufficient to establish the general, comprehensive viscosity model required for geochemical purposes. As a zeroth-order approximation, it is thus useful to consider how the viscosity of a molten rock is related to those of components less simple than oxides such as the normative mineral compositions (Figs. 7–8). For both our rhyolite and andesite compositions, $SiO_2$ is a normative component, but it is clear that the viscosity of pure $SiO_2$ is irrelevant for accounting for that of molten rocks because of its exceptionally high value. Of course, network-modifier cations have a tremendous depressing effect on the viscosity of $SiO_2$, and this is the reason why the viscosity of rhyolite and andesite does not differ greatly in spite of the significantly different $SiO_2$ contents of these melts. In contrast to the viscosity, the heat capacity is rather insensitive to the size of the constituting silicate units of the melt. Thus, the influence of the $SiO_2$ content of a melt is quite different for transport and thermodynamic properties.

The data plotted in Figs. 7 and 8 show that the high-temperature viscosities of rhyolite and andesite liquids fall within the range of those of their other mineral components. Of course, there are different ways these complex compositions can be recast in terms of a subset of arbitrary mineral components, excluding $SiO_2$. Regardless of this choice, it is clear that the high-temperature data can be approximated by appropriately making a weighted sum of the viscosities of these components. Such a model would not work at low temperatures, however, because the viscosity of these molten rocks is considerably lower than those of the end-members. This effect is similar to that described for simple systems whereby the entropy of mixing of substituting cations contributes so heavily to the total configurational entropy of mixed melts that these liquids have low-temperature viscosities several orders of magnitude lower than those of the end-members (e.g., Richet 1984; Richet and Bottinga 1984b; Neuville and Richet 1991). As a matter of fact, (Na, K) mixing is the likely reason why the viscosity of rhyolite becomes much lower than that of $NaAlSi_3O_8$ liquid at low temperatures, also reducing the deviations from Arrhenian variations.

Finally, it is well known that water is a component of rhyolite melts which can exert a profound influence on their rheological properties at a few weight percent level (Shaw 1963). Its influence on the thermodynamic properties is largely unknown and discussion of this role is beyond the scope of this work since we do not present any new data relevant to this problem. We will just emphasize that kbar pressures are needed to keep significant water solubilities, with the result that the calorimetric measurements possible at this moment (e.g., Clemens and Navrotsky 1987) do not have the accuracy required for heat capacity modeling.

*Acknowledgements.* We thank S. Nadeau for the vacuum fusion experiments; F. Guyot for the T.E.M. observations; M. Madon for comments; and especially J. Beckett and B.O. Mysen for their remarkably thorough reviews of this paper. Contribution CNRS-INSU-DBT 525.

## References

Adam G, Gibbs JH (1965) On the temperature dependence of cooperative relaxation properties in glass-forming liquids. J Chem Phys 43:139–146

Bacon CR (1977) High-temperature heat content and heat capacity of silicate glasses: experimental determination and a model for calculation. Am J Sci 277:109–135

Bockris JO' M, Lowe DC (1954) Viscosity and structure of molten silicates. Proc R Soc London A226:423–435

Bottinga Y, Weill DF (1970) Densities of liquid silicate systems calculated from partial molar volumes of oxide components Am J Sci 269:169–182

Bottinga Y, Weill DF (1972) The viscosity of magmatic liquids: a model for calculation. Am J Sci 272:438–475

Bowen NL (1928) The evolution of the igneous rocks. Dover Publications Inc, New York (Reprinted 1956)

Carmichael ISE, Nicholls J, Spera FJ, Wood BJ, Nelson SA (1977) High-temperature of silicate liquids: application to the equilibration and ascent of basic magma. Philos Trans R Soc London A 286:373–431

Carron JP (1969) Recherche sur la viscosité et les phénomènes de transport des ions alcalins dans les obsidiennes granitiques. Trav Lab Géol, n°3, Ec Norm Supér, Paris

Clemens JD, Navrotsky AN (1987) Mixing properties of $NaAlSi_3O_8$ melt-$H_2O$: new calorimetric data and some geological implications. J Geol 95:173–186

Cukierman M, Uhlmann DR (1973) Viscosity of liquid anorthite. J Geophys Res 78:4920–4923

Dingwell DB (1989) Effect of fluorine on the viscosity of diopside liquid. Am Mineral 74:333–338

Dingwell DB, Virgo D (1987) The effect of oxidation state on the viscosity of melt in the system $Na_2O$-FeO-$Fe_2O_3$-$SiO_2$. Geochim Cosmochim Acta 51:195–205

Hummel W, Arndt J (1985) Variation of viscosity with temperature and composition in the plagioclase system. Contrib Mineral Petrol 90:83–92

Klein LC, Fasano BV, Wu JM (1983) Viscous flow behavior of four iron-containing silicates with alumina, effects of composition and oxidation condition. J Geophys Res 88:A880–A886

Kress VC, Carmichael ISE (1988) The lime-iron-silicate melt system: redox and volume systematics. Geochim Cosmochim Acta 53:2883–2892

Lange RA, Navrotsky A (1992) Heat capacities of $Fe_2O_3$-bearing silicate liquids. Contrib Mineral Petrol 110:311–320

Leko BK (1979) Viscosity of vitreous silica. Fiz Khim Stekla 5:258–278

Lejeune AM, Richet P (1991) Rheology of magmas. Terra Abstr 3:445

Murase T, McBirney AR (1973) Properties of some common igneous rocks and their melts at high temperatures. Geol Soc Am Bull 84:3563–3592

Mysen BO (1988) Structure and properties of silicate melts. Elsevier, Amsterdam New York

Neuville DR, Richet P (1991) Viscosity and (Ca, Mg) mixing in molten pyroxenes and garnets. Geochim Cosmochim Acta 55:1011–1021

Newman S, Stolper EM, Epstein S (1986) Measurement of water rhyolitic glasses: calibration of an infrared spectroscopic technique. Am Mineral 71:1527–1541

Regnard IR, Chavez-Rivas F, Chappert J (1981) Study of the oxydation states and magnetic properties of iron in volcanic glasses: Lipari and Teotihuacan obsidians. Bull Minéral 104:204–210

Richet P (1984) Viscosity and configurational entropy of silicate melts. Geochim Cosmochim Acta 48:471–483

Richet P (1987) Heat capacity of silicate glasses. Chem Geol 62:111–124

Richet P, Bottinga Y (1984a) Glass transitions and thermodynamic properties of amorphous $SiO_2$, $NaAlSi_nO_{2n+2}$ and $KAlSi_3O_8$. Geochim Cosmochim Acta. 48:453–470

Richet P, Bottinga Y (1984b) Anorthite, andesine, diopside, wollastonite, cordierite and pyrope: thermodynamics of melting, glass transitions, and properties of the amorphous phases. Earth Planet Sci Lett, 67:415–432

Richet P, Bottinga Y (1985) Heat capacity of aluminum-free liquid silicates. Geochim Cosmochim Acta 49:471–486

Richet P, Bottinga Y (1986) Thermochemical properties of silicate glasses and liquids: a review. Rev Geophys 24:1–25

Richet P, Neuville DR (1992) Thermodynamics of silicate melts: configurational properties. Adv Phys Geochem 10:132–160

Richet P, Bottinga Y, Deniélou L, Petitet JP, Téqui C (1982) Thermodynamic properties of quartz, cristobalite and amorphous $SiO_2$: drop calorimetry measurements between 1000 and 1800 K and a review from 0 to 2000 K. Geochim Cosmochim Acta 46:2639–2658

Richet P, Robie RA, Hemingway BS (1986) Low-temperature heat capacity of diopside glass ($CaMgSi_2O_6$): a calorimetric test of the configurational entropy theory applied to the viscosity of liquid silicates. Geochim Cosmochim Acta 50:1521–1533

Richet P, Gillet P, Fiquet G (1992) Thermodynamic properties of minerals: macroscopic and microscopic approaches. Adv Phys Geochem 10:98–131

Shaw HR (1963) Obsidian-$H_2O$ viscosities at 1000 and 2000 bars in the temperature range 700 °C to 900 °C. J Geophys Res 68:6337–6343

Stebbins JF, Weill DF, Carmichael ISE, Moret LK (1982) High-temperature heat contents and heat capacities of liquids and glasses in the system $NaAlSi_3O_8$-$CaAl_2Si_2O_8$. Contrib Mineral Petrol 80:276–284

Stebbins JF, Carmichael ISE, Moret LK (1984) Heat capacities and entropies of silicates liquids and glasses. Contrib Mineral Petrol 86:131–148

Taylor TD, Rindone GE (1970) Properties of soda aluminosilicate glasses: V low-temperature viscosities. J Am Ceram Soc 53:692–695

Urbain G, Bottinga Y, Richet P (1982) Viscosity of liquid silica, silicates and aluminosilicates. Geochim Cosmochim Acta 46:1061–1071

Webb SL, Dingwell DB (1990a) Non-newtonian rheology of igneous melts at high stresses and strain rates: experimental results for rhyolite, andesite, basalt and nepheline J Geophys Res 95:15695–16701

Webb SL, Dingwell DB (1990b) The onset of non-newtonian rheology of silicate melts. Phys Chem Minerals 17:125–132

Editorial responsibility: W. Schreyer